Scientific Research Publishing

Journal of Power and Energy Engineering, 2024, 12, 31-47
https://www.scirp.org/journal/jpee
ISSN Online: 2327-5901
ISSN Print: 2327-588X

Thermal Decomposition of Olive-Solid Waste by TGA: Characterization and Devolatilization Kinetics under Nitrogen and Oxygen Atmospheres

Yahya H. Khraisha

Chemical Engineering Department, University of Jordan, Amman, Jordan
Email: khraisha@ju.edu.jo, y_khraisha@yahoo.com

How to cite this paper: Khraisha, Y.H. (2024) Thermal Decomposition of Olive-Solid Waste by TGA: Characterization and Devolatilization Kinetics under Nitrogen and Oxygen Atmospheres. *Journal of Power and Energy Engineering*, **12**, 31-47.
https://doi.org/10.4236/jpee.2024.123003

Received: February 4, 2024
Accepted: March 18, 2024
Published: March 21, 2024

Abstract

Despite the fact that a few countries in the Mediterranean and the Middle East have limited crude oil reserves, they have abundant biomass feedstocks. For instance, Jordan relies heavily on the importation of natural gas and crude oil for its energy needs; but, by applying thermochemical conversion techniques, leftover olive oil can be used to replace these energy sources. Understanding the chemical, physical, and thermal characteristics of raw materials is essential to obtaining the most out of these conversion processes. Thermogravimetric analysis was used in this study to examine the thermal behavior of olive-solid residue (kernel) at three different heating rates (5, 20 and 40 C/min) in nitrogen and oxygen atmospheres. The initial degradation temperature, the residual weight at 500 and 700˚C and the thermal degradation rate during the devolatilization stage (below 400˚C) were all determined. It was found that in N_2 and O_2 atmospheres, both the initial degradation temperature and the degradation rate increase with increasing heating rates. As heating rates increase in the N_2 atmosphere, the residual weight at 500 or 700˚C decreases slightly, but at low heating rates compared to high heating rates in the O_2 atmosphere, it decreases significantly. This suggests that a longer lignin oxidation process is better than a shorter one. Coats and Redfern approach was used to identify the mechanism and activation energy for the devolatilization stage of pyrolysis and oxidation reactions. The process mechanism analysis revealed that the model of first-order and second-order reactions may adequately describe the mechanism of heat degradation of the devolatilization step of olive-solid waste for pyrolysis and oxidation processes, respectively.

Keywords

Biomass, Olive-Solid Waste, Thermogravimetry, Pyrolysis, Oxidation, Heating Rates, Kinetics

1. Introduction

Jordan has struggled greatly in recent years to meet its energy needs because the majority of its energy needs were met by imported oil, natural gas, and petroleum products. Due to the enormous number of refugees it has taken in from nearby unstable nations, its population has been growing quickly to large numbers (from 5 to 11.3 million in the years 2000 and 2023, respectively [1]), which exacerbates its energy dilemma. New energy sources have emerged as a result of rising energy use and needs. However, common local energy sources including solar, wind, oil shale, and nuclear energy are currently being considered or some are already in use. Furthermore, Jordan has a lot of biomass resources, namely energy crops, farms, agricultural waste, municipal trash, and animal waste, which might help with the search for alternative energy sources, particularly in rural areas. The study's focus, olive cake, represents one of the most significant agricultural wastes.

In Jordan, the production of olive oil has become a significant agricultural industry, particularly in the north and center of the country. This is ultimately the result of the government's expansion strategy for olive tree agriculture, notably over the past two decades. More than 15 million olive trees are thought to exist throughout the nation, yielding about 100,000 tons of olive fruit per year [2]. Jordan now produces 24000 tons of olive oil annually, making it the eighth-largest producer of olive oil in the world [3]. The pressing or squeezing of the olives results in the production of olive oil as the primary product and olive cake as an additional or subsidiary product. The output of olive oil and olive cakes in Jordan from 2016 to 2021 is depicted in **Figure 1** [2]. It is obvious that 2019 had the highest production of oil and solid residues, at 35,000 and 53,000 tons, respectively. Moreover, **Figure 1** illustrates how production variation can be attributed to a number of variables. These variables include the amount of rain that falls each year, the conditions and methods used to extract olive oil, the age or modernity of the pressing equipment, and the quality of the olive fruits.

Thermochemical methods are frequently used to convert biomass waste into forms of usable energy. Combustion, pyrolysis, and gasification are the three main types of conversion processes that fall under this category, and they are all carried out at temperatures between 300 and 1500°C [4]. Due to the fact that olive cake burns cleanly and produces no sulfur oxides and little nitrogen oxides during combustion, it is possible to directly burn olive cake or co-burn it with coal or another biomass fuel. Fluidized bed methods have shown efficient ways to transform waste solid biomass, like olive cake, into usable energy [5] [6] [7]. For

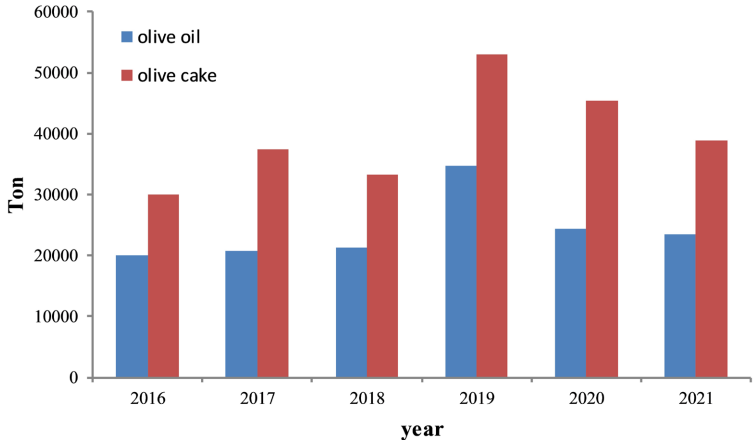

Figure 1. Olive oil and olive cake quantities per year.

example, Khraisha *et al.* [7] have studied the combustion behavior of Jordanian olive cake in a fluidized bed combustor at different operating conditions. They have found that olive cake can be continuously burned like most solid fuels with a combustion efficiency of 80 - 90%.

Olive solid wastes are pyrolyzed to produce a variety of energy products, including solid char, liquid oils, and gases. The quantity and quality of the finished products are significantly influenced by the temperature and heating rates. In order to maximize liquid oils, for instance, low temperature and high heating rates are chosen, whereas high temperature and low heating rates are chosen in order to obtain significant amounts of gaseous fuel [8] [9]. Gasification is a conversion process that transforms organic materials into primary permanent gases with char, water, and condensable as byproducts at high temperatures and reduced conditions. It was found [10] [11] that the fluidized bed technique offers a good way to convert waste solid material into useful gaseous products at temperatures that are not very high. This is achieved by gasifying or co-gasifying waste materials with low-quality coal.

A well-known method for examining the thermochemical behavior of solid carbonaceous material, such as coal, oil shale, and biomass, is the thermogravimetric analyzer (TGA) [12] [13] [14]. Both dynamic (non-isothermal) and static (isothermal) TGA methods were employed to gather information for reaction kinetics or to forecast the thermal degradation of tested samples. However, each one has special advantages and disadvantages, but as a whole, they provide useful information that helps in developing an appropriate design for commercial thermochemical convertors.

The study aimed to: (a) perform a thermogravimetric analysis in nitrogen and oxygen atmospheres at three different heating rates (5, 20, and 40 °C/min) on a waste solid sample of olive oil from Jordan; (b) determine the thermal degradation, initial degradation temperature, and residual weights at 500 and 700°C for this olive-solid waste sample; and (c) examine the TGA data at the devolatilization stage using the Coats and Redfern model to determine the kinetic parameters and the nature of the mechanism.

Figure 2. Olive solid residues before and after grinding.

Table 1. Physical and chemical properties of olive-solid residues.

Proximate analysis				Ultimate analysis					HHV[a], kJ/kg	H/C atomic ratio	(A/F)[b] kg_{air}/kg_{fuel}
M	VM	F.C	A	C	H_2	N_2	S	O_2	18034	1.61	5.67
4.8	80.2	10.3	4.7	48.6	6.5	1.7	0.0	43.2			

[a]Dulong formula, [b]Based on mass balance calculations.

2. Experimental and Methods

2.1. Sample Preparation

Following the collection of the olive fruit from the Jordanian market, the samples of olive residue was produced and prepared. The raw olive solid residues are shown in Figure 2 (on the left). These residues were cleaned, washed with water, and then allowed to air dry. The solid residue samples were then crushed, sieved to a mesh size of less than 250 μm, and stored in a desiccator for later processing. The crushed sample is shown in Figure 2 on the right side.

2.2. Physical and Chemical Analysis

The physical and chemical characteristics of olive residues were analyzed according to standard methods. Table 1 shows the proximate, ultimate analyses, and calorific value of solid olive residue.

2.3. Thermogravimetric Analysis

Olive-solid residue samples of about 10 mg were thermally investigated using the mogavimetric analysis in N_2 and O_2 atmospheres at three heating rates (5, 20, 40 °C/min) from ambient temperature to 1000°C. The experiments were performed in a Netzsch STA 409 PC Luxx thermal analyzer.

2.4. Kinetic Approach

The thermal decomposition of solid material may be represented by the following reaction [15] [16] [17]:

$$A(solid) \rightarrow B(volatile) + C(solid) \quad (1)$$

For dynamic TG experiments at constant heating rate of temperature change, $\alpha = dT/dt$, the rate of conversion, dx/dt, may be written as:

$$\frac{dx}{dt} = A\exp\left(-\frac{E}{RT}\right) f(x) \tag{2}$$

where:

A: Arrhenius factor,

E: activation energy,

R: gas constant,

T: degradation temperature,

t: reaction time,

x: fraction decomposed of the sample at time t, and is described as:

$$x = \frac{w_0 - w}{w_0 - w_f} \tag{3}$$

w_0, w_f: initial and final weight of the sample during the TG experiments,

w: weight of the sample at time t,

$f(x)$: conversion function. For example, $(1 - x)$ for the first order reaction.

Integration of equation 2 leads to the general formula of Coats-Redfern [15]:

$$\ln\left(\frac{g(x)}{T^2}\right) = \ln\frac{AR}{\alpha E} - \frac{E}{RT} \tag{4}$$

where $g(x)$ is the integrated form of the conversion function $f(x)$. According to the reaction mechanism, this function, $g(x)$, is commonly given in literature [15] [16]. **Table 2** summarizes all possible functions and mechanisms. E and A kinetic-parameters can be obtained from the curve of line drawn from the lift side

Table 2. Reaction mechanisms, $f(x)$ and $g(x)$ forms for thermal solid decomposition reaction [15] [16].

Model	Mechanism	$f(x)$	$g(x)$
1	First-order reaction	$(1 - x)$	$-\ln(1 - x)$
2	Second-order reaction	$(1 - x)^2$	$(1 - x)^{-1} - 1$
3	Third-order reaction	$(1 - x)^3$	$[(1 - x)^{-2} - 1]/2$
4	Power law (P2)	$2x^{1/2}$	$x^{1/2}$
5	Power law (P3)	$3x^{2/3}$	$x^{1/3}$
6	Power law (P4)	$4x^{3/4}$	$x^{1/4}$
7	One-dimensional Diffusion (D1)	$1/2x$	x^2
8	Contracting area (R2)	$2(1 - x)^{1/2}$	$[1 - (1 - x)^{1/2}]$
9	Contracting volume (R3)	$3(1 - x)^{2/3}$	$[1 - (1 - x)^{1/3}]$
10	Two-dimensional Diffusion (D2)	$[-\ln(1 - x)]^{-1}$	$[(1 - x)\ln(1 - x)] + x$
11	Three-dimensional Diffusion (D3)	$3(1 - x)^{2/3}/[2(1 - (1 - x)^{1/3})]$	$[1 - (1 - x)^{1/3}]^2$
12	Ginstling-Brounshtein (D4)	$3/2((1 - x)^{-1/3} - 1)$	$(1 - (2x/3) - (1 - x)^{2/3})$
13	Avarami-Erofe'ev (A2)	$2(1 - x)[-\ln(1 - x)]^{1/2}$	$[-\ln(1 - x)]^{1/2}$
14	Avarami-Erofe'ev (A3)	$3(1 - x)[-\ln(1 - x)]^{2/3}$	$[-\ln(1 - x)]^{1/3}$
15	Avarami-Erofe'ev (A4)	$4(1-x)[-\ln(1 - x)]^{3/4}$	$[-\ln(1 - x)]^{1/4}$

of equation 4 against 1/T. The slope of the line gives E and the point of intersection A. However, in order to specify the most probable model, all mechanisms in Table 2 were fitted to TG experimental data.

3. Results and Discussion

3.1. Proximate Analysis

The proximate analysis of the sample of olive-solid residue is presented in Table 1. It is clear to see that the olive residue contains a lot of volatile organic matter (84 wt%, on a dry basis), which can be converted into gas and oil during pyrolysis. In addition, under high temperature (700 - 900°C) conditions, the residue could be used as a feedstock for a gasification or combustion process. The tested sample's percentage of volatile matter generally falls within the range of biomass and wood materials [18].

3.2. Ultimate Analysis and Heating Value

The ultimate analysis of the sample of olive residue is also shown in Table 1. The tested olive residue was found to have a composition that is similar to other biomass waste materials [19] [20]. However, because the amount of sulfur is so small, there won't be any significant environmental effects from using this material in a thermal application. The nitrogen value of 1.6% indicates the ability of the sample to cause the emission of NO_x on combustion [21]. In general, the air-to-fuel ratio and the heating value can both be calculated using the data from elemental analysis. To calculate the heating value, one can use the Dulong formula or any other empirical equation [22] [23]. The air-to-fuel mass ratio and the higher heating value were calculated using material balance calculations, Dulong formula and were found to be 5.67 and 18,034 kJ/kg, respectively. According to this, olive waste material has a higher energy throughput than, for instance, lignite coals (HHV: 5.5 - 14.5 MJ/kg [22]). Generally speaking, the calculated HHV value of the olive solid waste sample is in the range of 18 to 23 MJ/kg of the heating values of olive pit and leftover olive cake [21] [23] [24]. Based on the overall average production of 40,000 tons of olive mill solid waste (estimated from Figure 1), in a simplified preliminary approach, an overall annual energy potential of 4.0 10^4 x 18.03 GJ, i.e. ca. 72.14 10^4 GJ or ca. 200 GWh. This is annual potential resources would be equivalent to about 1.7 10^4 of TOE (ton of oil equivalent).

3.3. Thermal Analysis of Olive-Solid Residue

Figures 3(A), 3(B) and 3(C) and Figures 4(A), 4(B) and 4(C) illustrate the TG and DTG thremograms of olive residue sample heated at 5, 20 and 40 °C/min, under N_2 and O_2 atmospheres, respectively. Similar profiles were reported for olive solid wastes by Chouchene *et al.* [25], Ducom *et al.* [26] and Gomez-Martin *et al.* [27]. The TG figures reveal a small weight decrease (2 - 3%) at 100 to 200°C, which is possibly due to evaporation of moisture and or less volatile components. After that, the TG curves have shown three mass losses through the

temperature 200 to 800°C region. The first sharp drop in the weight of the sample with peaks (DTG curves) around 258, 277, 292°C for 5, 20, 40 °C/min in N_2 and O_2 atmospheres, respectively (**Figure 3** and **Figure 4**), are attributed for the decomposition of hemicellulose [28] [29] [30]. The next weight drop at higher temperature with peaks (DTG curves) around 320 - 345°C region for both O_2 and N_2 atmospheres (**Figure 3** and **Figure 4**), are attributed to cellulose decomposition [28] [29] [30]. These two weight drops which take place below 400°C are called devolatilization stage [25]. Thereafter a slow pyrolysis and oxidation occurs over a large temperature range until 900°C for N_2 and O_2 atmospheres, respectively, as shown in **Figure 3** and **Figure 4**. The slow reactions are attributed to the lignin thermal decomposition (N_2 atmosphere) or oxidation (O_2 atmosphere) [31]. As indicated by other investigator [32], higher heating rates increase DTG peaks, as individual devolatilization peaks overlap as well as this caused the disappearance of the second peak as shown in **Figure 4(C)** at 40 °C/min.

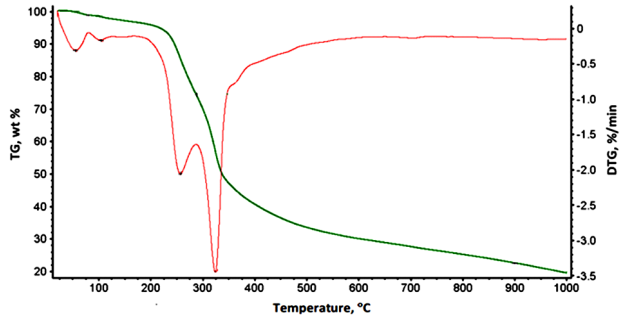

(A)

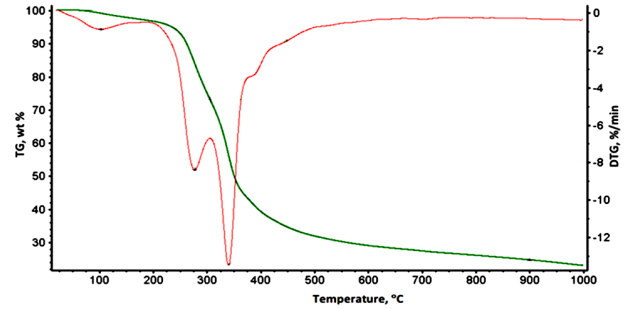

(B)

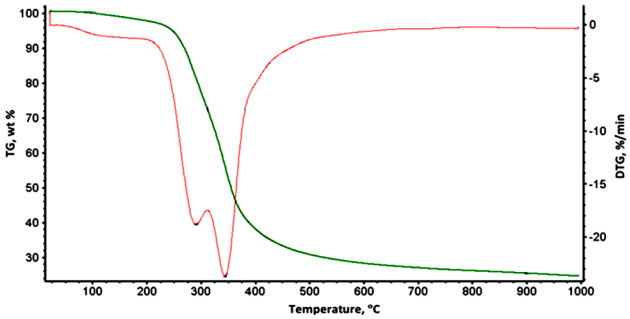

(C)

Figure 3. A. TG and DTG at 5 °C/min under N_2 atmosphere; B. TG and DTG at 20 °C/min under N_2 atmosphere; C. TG and DTG at 40 °C/min under N_2 atmosphere.

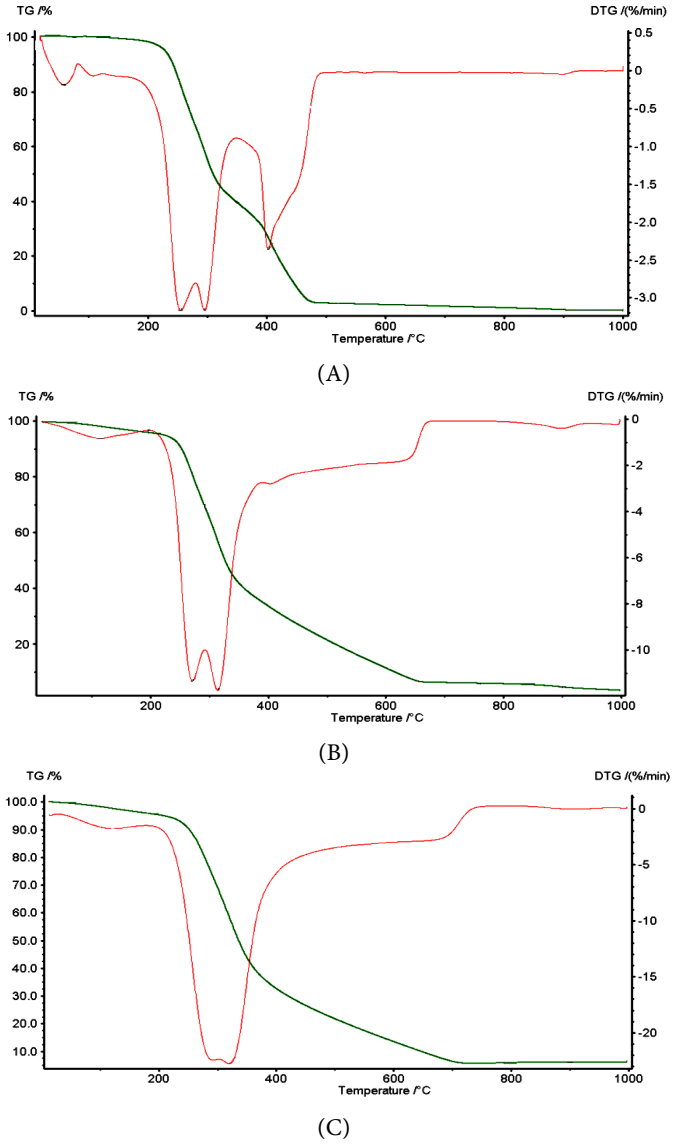

Figure 4. (A) TG and DTG at 5 °C/min under O_2 atmosphere; (B) TG and DTG at 20 °C/min under O_2 atmosphere; (C) TG and DTG at 40 °C/min under O_2 atmosphere.

3.4. Thermal Degradation Rate

As can be seen in **Figures 5(A) and 5(B)**, the rate of thermal degradation rose as the heating rate increased for both the hemicellulose and cellulose breakdown of olive solid residues in N_2 and O_2 atmospheres. When cellulose is pyrolyzed in a nitrogen atmosphere, the rate of thermal degradation increases more than when hemicellulose decomposes. By contrast, the rate of thermal degradation for both cellulose and hemicellulose components nearly remains constant in an oxygen atmosphere, as illustrated in **Figures 5(A) and 5(B)**. It's interesting to observe that, for both tested N_2 and O_2 atmospheres, the degradation rate increases with increasing heating rate from 5 to 20 ˚C/min by about 4 times, while at 40 °C/min, it increases by about 2 times. It can be concluded that a strong evolution toward volatile components and a high conversion rate of some heavy compo-

nents to light species may be linked to the abrupt change in temperature from low to high. This informs that the olive residue is more easily thermochemical degradable at high heating rate than low one. This finding has been supported by other investigators [28] [29] [30] [33] who found that the rate of thermal degradation of biomass samples is directly proportional to the subjected heating rate.

Figure 6 displays the initial temperatures of thermal degradation for the sample of olive-solid residue that was tested. Under O_2 atmosphere, the initial temperature of degradation of olive-solid residue is slightly greater than under N_2 atmosphere. Generally speaking, as the heating rate rises, so does the initial degradation temperature. This finding suggests that the starting temperature of devolatilization of olive oil residue is considerably impacted by an increase in heating rate. Other researchers noted similar findings with biomass materials [29] [30].

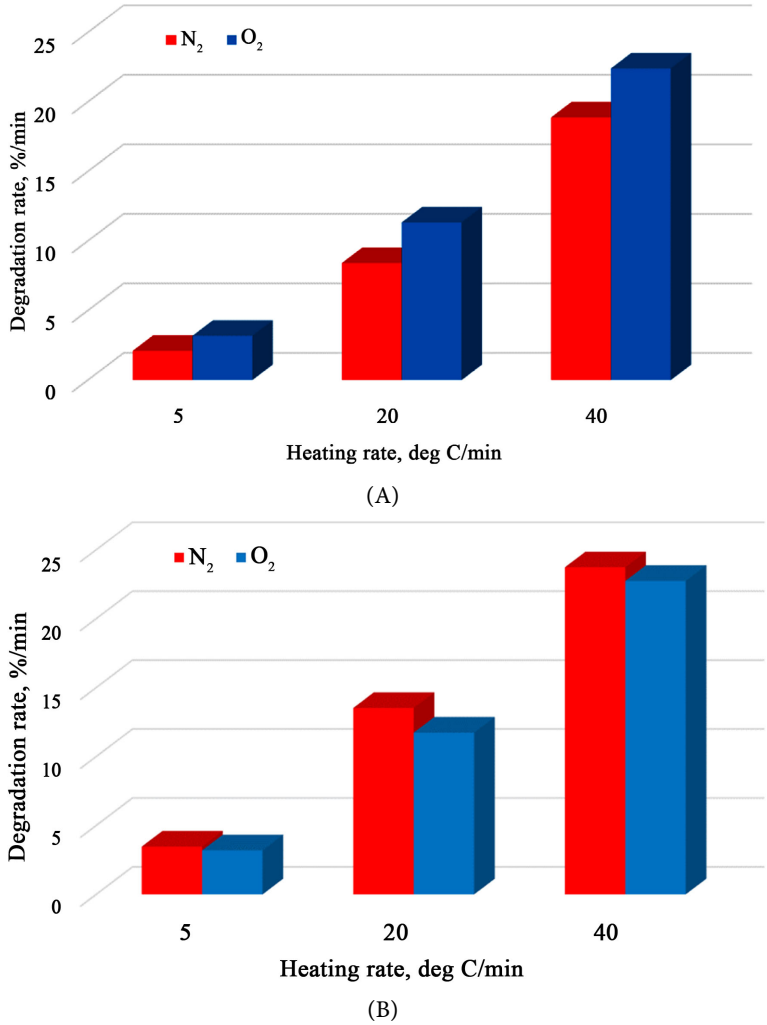

Figure 5. (A) Thermal degradation rate for hemicellulose decomposition of olive solid residue under N_2 and O_2 atmospheres. (B) Thermal degradation rate for cellulose decomposition of olive solid residue under N_2 and O_2 atmospheres.

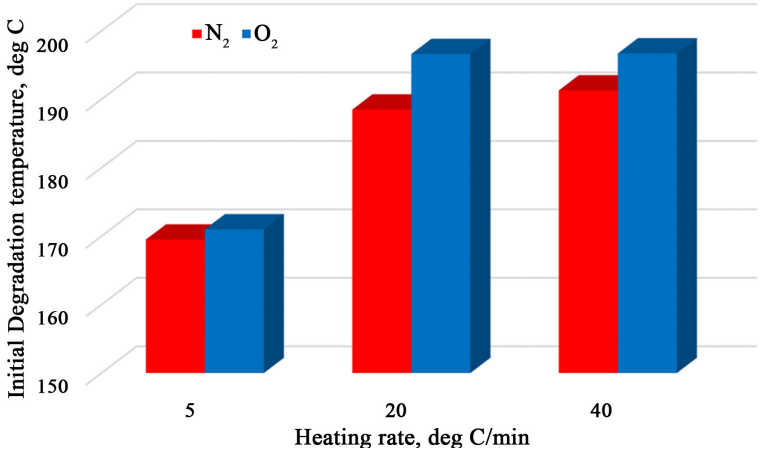

Figure 6. Initial degradation temperature for the decomposition of olive solid residue in N_2 and O_2 atmospheres.

3.5. Residual Weight at 500 and 700°C

While combustion occurs at temperatures above 600°C, pyrolysis of biomass is typically carried out at or above 500°C. Therefore, two temperatures, 500 and 700°C are chosen to compare the residual weight percent at different heating rates and atmospheres (N_2 and O_2). The residual weight of the olive-solid residue sample under N_2 and O_2 atmospheres is displayed in Figure 7 at 500 and 700°C at three different heating rates of 5, 20, and 40 °C/min. As previously mentioned, Figure 3 and Figure 4 demonstrate how thermally and chemically highly reactive the three components of lignocellulosic materials (hemicellulose, cellulose and lignin) were in the 200 - 500°C temperature range.

The residual weight at 500 and 700°C is nearly constant at the three tested heating rates under N_2 atmosphere (Figure 7). When biomass is pyrolyzed without oxygen, gases, liquid (bio-oil), and solid (bio-char) are the end products. 500°C is the optimum pyrolysis temperature for bio-oil production [34] [35]. A typical biomass feedstock produces 15 to 30 weight percent solid biochar material under these conditions. As illustrated in Figure 7 for N_2 atmosphere conditions, the pyrolysis of the solid waste sample from the olives in this study yielded a solid weight residue of roughly 31 to 33 wt% at 500°C. Other researchers noted similar residual weight percentages for olive-solid waste that was thermally decomposed in an inert atmosphere [25] [26].

The residual weight is highly influenced by the heating rate under O_2 atmosphere or combustion process, especially at low heating rates. In contrast to about 22 wt% at 20 or 40 °C/min, the residual weight, for instance, drops to approximately 3 wt% at 5 °C/min at 500 C. This suggests that a longer lignin oxidation process is preferred over a shorter one. Table 3, on the other hand, provides an overview of the solid waste sample's combustion thermal properties. The profiles of the sample (DTG) shown in Figure 4 are used to determine the combustion properties. It's interesting to note that when the heating rate was increased, both the burn out temperature and the maximum rate of combustion (percent weight

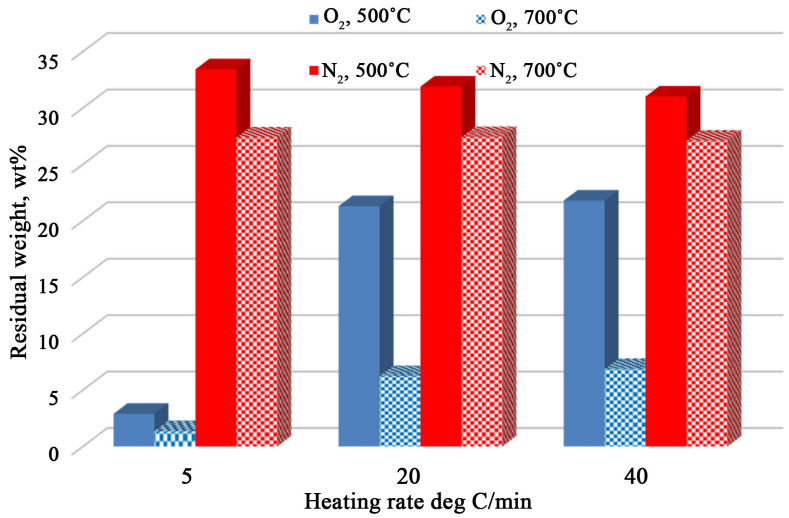

Figure 7. Residual weight at 500 and 700°C for the decomposition of olive solid residue in N_2 and O_2 atmospheres.

Table 3. Combustion properties of the olive-solid waste sample.

Heating rate, °C/min	5	20	40
Initial temperature, °C	184	210	208
Peak temperature, °C	255	272	290
Burnout temperature, °C	493	675	749
Max combustion rate, %/min	3.17	11.32	22.34

loss/min) increased. For residual olive cake analyzed under air atmosphere and heating rate at 30 °C/min, Miranda *et al.* [21] have shown values of burnout temperature, initial degradation temperature, and maximum combustion rate that are very close to ones obtained for the analyzed sample.

3.6. Kinetics

Solid waste samples derived from olive oil were typically subjected to three primary stages of pyrolysis or oxidation. The devolatilization stage, which is the second step following moisture removal, is defined as the breakdown of hemicelluloses and cellulose in section 3.3. The final step is the very slow breakdown of lignin over a wide temperature range (above 400°C). Only the second stage of the process—the devolatilization step—which is crucial to the gasification, bio-oil production, and combustion processes—is subjected to kinetic analysis in this study. Furthermore, the solid waste's thermal conversion at this point reaches between 52 and 60 weight percent, which is significant for kinetic analysis.

Regression coefficients of 15 different reaction mechanisms (Table 2) were obtained graphically and tabulated in Table 4 and Table 5 for the devolatilization step. According to Table 4, first order reaction mechanism was fitted to TGA experimental data conducted in N_2 atmosphere. Figure 8 provides an illustration of the Coats Redfern procedure's graphical method for Model 1. This mechanism was used to calculate the activation energies and Arrhenius factors

for the devolatilization step for each of the three heating rates. The results are displayed in Table 6. The apparent activation energies are somewhat dependent on the heating rate. Nevertheless, it was found that the activation energy required to devolatilize waste samples made of solid olive oil ranged from 47 to 85 kJ/mol. This result reveals that the reactivity of thermal decomposition reactions was only slightly affected by changes in heating rates (5, 20, 40 °C/min). These outcomes are consistent with those of A. Chouchene *et al.* [25] for the devolatilization stage of solid waste from olives in an inert atmosphere. On the other hand, different activation energies were demonstrated by other researchers [36] [37]. The variation in olive-solid waste samples' composition, the type of experimental technique employed, and the kinetic model applied could all be contributing factors to the difference.

Table 4. Regression coefficients of olive-solid waste samples for devolatilization step under N_2 atmosphere.

Model	R^2		
	5 °C/min	20 °C/min	40 °C/min
1	**0.9727**	**0.9734**	**0.9830**
2	0.9433	0.9513	0.9817
3	0.8803	0.8891	0.9376
4	0.8545	0.8827	0.8669
5	0.7755	0.8337	0.7987
6	0.6320	0.7534	0.6784
7	0.9161	0.9256	0.9217
8	0.9861	0.9520	0.9533
9	0.9598	0.9614	0.9653
10	0.9422	0.9467	0.9463
11	0.9653	0.9661	0.9703
12	0.9515	0.9543	0.9554
13	0.9639	0.9658	0.9768
14	0.9505	0.9549	0.9670
15	0.9288	0.9385	0.9510

Table 5. Regression coefficients of olive-solid waste samples for devolatilization step under O_2 atmosphere.

Model	R^2		
	5 °C/min	20 °C/min	40 °C/min
1	0.9509	0.9455	0.9610
2	**0.9890**	**0.9926**	**0.9978**
3	0.9761	0.9803	0.9775
4	0.8027	0.7923	0.7690
5	0.7339	0.7203	0.6274
6	0.6322	0.6154	0.3861
7	0.8680	0.8613	0.8762
8	0.9055	0.8967	0.9108
9	0.9222	0.9141	0.9293
10	0.8979	0.8902	0.9065

Continued

11	0.9307	0.9239	0.9409
12	0.9099	0.9022	0.9190
13	0.9381	0.9303	0.9433
14	0.9202	0.9088	0.9135
15	0.8945	0.8774	0.8591

Table 6. Kinetic parameters calculated based on the Coats & Redfern.

Heating rate, °C/min	N_2 atmosphere		O_2 atmosphere	
	E, kJ/mol	A, min^{-1}	E, kJ/mol	A, min^{-1}
5	47.1	6.1×10^5	119.9	8.6×10^{10}
20	85.3	1.8×10^7	117.4	5.7×10^{10}
40	77.5	4.8×10^6	92.5	2.6×10^8
Model	First-order reaction		Second-order reaction	

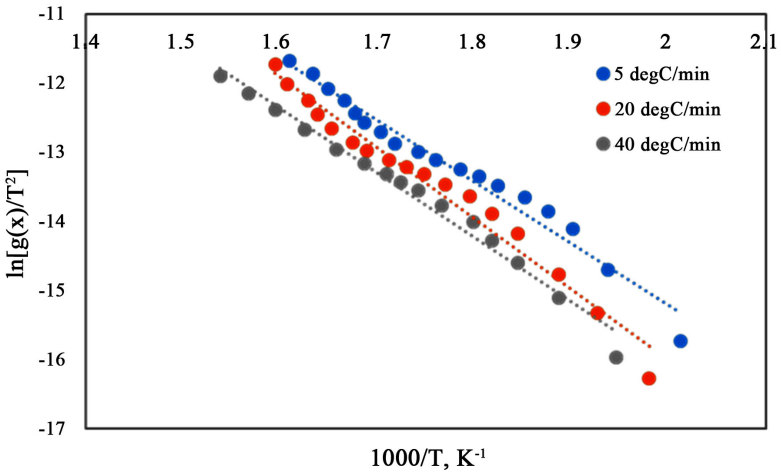

Figure 8. Plot of ln $[g(x)/T^2]$ against 1/T (model 1) for olive-solid waste decomposition under N_2 atmosphere.

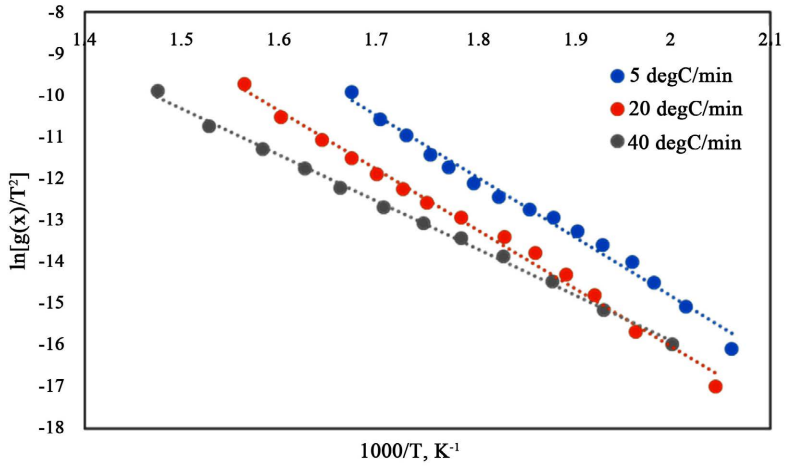

Figure 9. Plot of ln $[g(x)/T^2]$ against 1/T (model 2) for olive-solid waste decomposition under O_2 atmosphere.

The experimental TGA data collected in an O_2 atmosphere underwent the same analysis. The regression coefficients for the devolatilization step under an O_2 atmosphere are displayed in Table 5 for olive-solid waste samples. It is evident that the second order mechanism was fitted to the experimental data. Figure 9 provides an illustration of the Coats Redfern procedure's graphical method for Model 2. This mechanism was used to calculate the activation energies and Arrhenius factors for the devolatilization step for each of the three heating rates. The results are displayed in Table 6. Once more, the apparent activation energies are not significantly affected by heating rates (5 and 20 °C/min). The devolatilization of olive-solid waste samples under an O_2 atmosphere was found to require an activation energy that generally ranged from 93 to 120 kJ/mol. A. Chouchene *et al.* [25] reported activation values ranging from 55 to 100 kJ/mol for the devolatilization step of olive solid waste decomposed under oxidative atmosphere (10% and 20% O_2 concentration). J. Jauhininea *et al.* [36] reported that the devolatilization of olive-solid waste in an oxidative atmosphere had an activation energy value of 154 kJ/mol. M. Wzorek *et al.* [38] reported that samples of waste from olive mills that decomposed in an air atmosphere had an average activation value of between 130 and 139 kJ/mol. Several kinetic models were used to compute the activation energy values.

4. Conclusion

Thermal degradation experiments of olive-solid waste were performed under nitrogen and oxygen atmospheres at different heating rates of 5, 20, and 40 °C/min in temperature range from 25 to 1000°C. From the thermal degradation results, we can observe that the pyrolysis and oxidation processes occur in three steps drying, removal of volatiles and char conversion. In general, the TG curves showed two main mass losses. The first one is enclosed in the region of about 170 to 400°C which represents the hemicellulose and cellulose conversion and is confirmed by two peaks on DTG curves whilst the second loss occurs at high temperature above 390 °C for lignin conversion. The initial degradation temperature and the degradation rate increase with the increase of heating rates in N_2 and O_2 atmospheres. The residual weight at 500 or 700°C decreases slightly with the increase of heating rates in the N_2 atmosphere, but at low heating rates compared to high heating rates in the O_2 atmosphere, it decreases significantly. Nevertheless, after pyrolysis, the tested samples produced residual biochar weights of between 27 and 30 weight percent, which is comparable to the weight of a normal biomass feedstock. The devolatilization of an olive-solid waste sample is a first-order reaction in a nitrogen atmosphere and a second-order reaction in an oxygen atmosphere, according to data from kinetic analysis and experimentation. It was found that the activation energy values for pyrolysis and combustion ranged from 47 to 85 kJ/mol and 93 to 120 kJ/mol, respectively, during the devolatilization step. In conclusion, the outcomes acquired in nitrogen and oxygen environments could offer more beneficial data for biomass gasification and combustion processes, offering a more comprehensive and detailed explanation

of the pyrolysis and oxidation mechanisms.

Acknowledgements

The author would like to thank Ms. Arwa Sandouqa for her invaluable assistance with the chemical analysis and sample preparation. The author also expresses gratitude to the University of Jordan's Chemistry Department for granting permission to use its laboratory facilities.

Conflicts of Interest

The author declares no conflicts of interest regarding the publication of this paper.

References

[1] (2024) Jordan Population. https://www.worldometers.info/world-population/jordan-population/

[2] Department of Statistics (2023) Ministry of Agriculture, Annual Reports. Amman, Jordan. https://dosweb.dos.gov.jo/ar/agriculture/

[3] (2024) https://familyinjordan.com/en/2019/10/17/olive-oil-production-in-jordan-pay-visit-to-a-press/

[4] Hodge, B.K. (2017) Alternative Energy Systems and Applications. 2nd Edition, John Wiley & Sons, New York.

[5] Atimtay, A.T. and Varol, M. (2007) Investigation of Co-Combustion of Coal and Olive Cake in a Bubbling Fluidized Bed with Secondary Air Injection. *Fuel*, **88**, 10000-10008. https://doi.org/10.1016/j.fuel.2008.11.030

[6] Cliffe, K.R and Patumsawad, S. (2001) Co-Combustion of Waste from Olive Oil Production with Coal in a Fluidized bed. *Waste Management*, **21**, 49-53. https://doi.org/10.1016/S0956-053X(00)00057-X

[7] Khraisha, Y.H., Hamdan, M.A. and Qalalweh, H.S. (1999) Direct Combustion of Olive Cake Using Fluidized Bed Combustor. *Energy Sources*, **21**, 319-327. https://doi.org/10.1080/00908319950014803

[8] Demirbas, A. (2008) Producing Bio-Oil from Olive Cake by Fast Pyrolysis. *Energy Sources*, *Part A*: *Recovery*, *Utilization*, *and Environmental Effects*, **30**, 38-44. https://doi.org/10.1080/00908310600626747

[9] Uzum, B.B., Pütün, A.E. and Pütün E. (2007) Rapid Pyrolysis of Olive Residue. 1. Effect of Heat and Mass Transfer Limitations on Product Yields and Bio-Oil Composition. *Energy and Fuels*, **21**, 1768-1776. https://doi.org/10.1021/ef060171a

[10] Gómez-Barea, A., Arjona, R. and Ollero, P. (2005) Pilot-Plant Gasification of Olive Stone: A Technical Assessment. *Energy and Fuels*, **19**, 598-605. https://doi.org/10.1021/ef0498418

[11] Skonlon, V., Koufodimos, G., Samaras, Z. and Zabaniotou, A. (2008) Low Temperature Gasification of Olive Kernels in a 5-kW Fluidized Bed Reactor for H_2-Rich Producer Gas. *International Journal of Hydrogen Energy*, **33**, 6515-6524. https://doi.org/10.1016/j.ijhydene.2008.07.074

[12] Khraisha, Y.H. and Shabib, I.M. (2002) Thermal Analysis of Shale Oil Using Themogravimetry and Differential Scanning Calorimetry. *Energy Conversion Man-*

agement, **43**, 229-239. https://doi.org/10.1016/S0196-8904(01)00023-1

[13] Elmay, Y., Jeguirim, M., Trouvé, G. and Said, R. (2016) Kinetic Aanalysis of Thermal Decomposition of Date Palm Residues Using Coats-Redfern Method. *Energy Sources*, *Part A*: *Recovery*, *Utilization*, *and Environmental Effects*, **38**, 1117-1124. https://doi.org/10.1080/15567036.2013.821547

[14] Yan, J., Yang, Q., Zhang, L., Lei, Z., Li, Z., Wang, Z., Pen, S., Kang, S. and Shui, H. (2020) Investigation of Kinetics and Thermodynamic Parameters of Coal Pyrolysis with Model-Free Fitting Methods. *Carbon Resources Conversion*, **3**, 173-181. https://doi.org/10.1016/j.crcon.2020.11.002

[15] Brown, M.E. (2001) Introduction to Thermal Analysis: Techniques and Applications, 2nd Edition, Springer, New York.

[16] Aboulkas, A., El Harfi, K., El Bouadili, A., Benchanaa, M., Mokhlisse, A. and Outzourit, A. (2007) Kinetics of Co-Pyrolysis of Tarfaya (Morocco) Oil Shale with High Density Polyethylene. *Oil Shale*, **24**, 15-33. https://doi.org/10.3176/oil.2007.1.04

[17] Slopiecka, K., Bartocci, P. and Fantozzi, F. (2012) Thermogravimetric Analysis and Kinetic Study of Poplar Wood Pyrolysis. *Applied Energy*, **97**, 491-497. https://doi.org/10.1016/j.apenergy.2011.12.056

[18] Gaur, S. and Reed, T. (1998) Thermal Data for Natural and Synthetic Fuels. Marcel Dekker, Inc., New York.

[19] Volpe, R., Messineo, A., Millan, M., Volpe, M. and Kandiyoti, R. (2015) Assessment of Olive Waste as Energy Source: Pyrolysis, Torrefaction and the Key Role of H Loss in Thermal Breakdown. *Energy*, **82**, 119-127. https://doi.org/10.1016/j.energy.2015.01.011

[20] Blázquez, G., Caleo, M., Martinez-Garcia, C., Cotes, M.T., Ronda, M. and Marti'n-Lara, M.A. (2014) Characterization and Modeling of Pyrolysis of Two-Phase Olive Mill Solid Waste. *Fuel Processing Technology*, **126**, 104-111. https://doi.org/10.1016/j.fuproc.2014.04.020

[21] Miranda, T., Esteban, A., Rojas, S., Montero, I. and Ruiz, A. (2008) Combustion Analysis of Different Olive Residues. *International Journal of Molecular Sciences*, **9**, 512-525. https://doi.org/10.3390/ijms9040512

[22] Culp, A.W. (1991) Principle of Energy Conversion. 2nd Edition, McGraw-Hill, New York.

[23] Ouazzane, H., Laajine, F., El Yamani, M., El Hilaly, J., Rharrabti, Y., Amarouch, M.Y. and Mazouzi, D. (2017) Olive Mill Solid Waste Characterization and Recycling Opportunities: A Review. *Journal of Materials and Environmental Sciences*, **8**, 2632-2650. http://www.jmaterenvironsci.com/

[24] Khraisha, Y.H. (2022) Energetic Study on Jordanian Olive Cake and Woody Biomass Materials. *Journal of Power and Energy Engineering*, **10**, 1-13. https://doi.org/10.4236/jpee.2022.102001

[25] Chouchene, A., Jeguirim, M., Khiari, B., Zagrouba, F. and Trouvé, G. (2010) Thermal Degradation of Olive Solid Waste: Influence of Particle Size and Oxygen Concentration. *Resources*, *Conservation and Recycling*, **54**, 271-277. https://doi.org/10.1016/j.resconrec.2009.04.010

[26] Ducom, G., Gautier, M., Pietraccini, M., Tagutchou, J.P., Lebouil, D. and Gourdon, R. (2020) Comparative Analyses of Three Olive Mill Solid Residues from Different Countries and Processes for Energy Recovery by Gasification. *Renewable Energy*, **145**, 180-189. https://doi.org/10.1016/j.renene.2019.05.116

[27] Gomez-Martin, A., Chacartegui, R., Ramirez-Rico, J. and Martinez-Fernandez, J.

(2018) Performance Improvement in Olive Stone's Combustion from a Previous Carbonization Transformation. *Fuel*, **228**, 254-262. https://doi.org/10.1016/j.fuel.2018.04.127

[28] Nassar, M.M. (1988) Thermal Analysis Kinetics of Bagasse and Rice Straw. *Energy Sources*, **20**, 831-837. https://doi.org/10.1080/00908319808970101

[29] Örfao, J.J.M., Antunes, F.J.A. and Figueiredo, J.L. (1999) Pyrolysis Kinetics of Lignocellulosic Materials—Three Independent Reactions Model. *Fuel*, **78**, 349-358. https://doi.org/10.1016/S0016-2361(98)00156-2

[30] García-Ibañez, P., Sánchez, M. and Cabanillas, A. (2006) Thermogravimetric Analysis of Olive-Oil in Air Atmosphere. *Fuel Processing Technology*, **87**, 103-107. https://doi.org/10.1016/j.fuproc.2005.08.005

[31] Brebu, M. and Vasile, C. (2010) Thermal Degradation of Lignin—A Review. *Cellulose Chemical Technology*, **44**, 353-363. https://www.researchgate.net/publication/237090542_Thermal_degradation_of_lignin_-_A_Review#fullTextFileContent

[32] Jankovic, B., Radojevic, M.B., Balac, M., Stojiljkovic, D.D. and Manic, N.G. (2020) Thermogravimetric Study on the Pyrolysis Kinetic Mechanism of Waste Biomass from Fruit Processing Industry. *Thermal Science*, **24**, 4221-4239. https://doi.org/10.2298/TSCI200213191J

[33] Mansaray, K.G. and Ghaly, A.E. (1998) Thermal Degradation of Rice Husks in Nitrogen Atmosphere. *Bioresource Technology Journal*, **65**, 13-20. https://doi.org/10.1016/S0960-8524(98)00031-5

[34] Guedes, R.E., Luna, A.S. and Torres, A.R. (2018) Operating Parameters for Bio-Oil Production in Biomass Pyrolysis: A Review. *Journal of Analytical and Applied Pyrolysis*, **129**, 134-149. https://doi.org/10.1016/j.jaap.2017.11.019

[35] Mourant, D., Lievens, C., Gunawan, R., Wang, Y., Hu, X., Wu, L., Syed-Hassan, S.S.A. and Li, C.Z. (2013) Effects of Temperature on the Yields and Properties of Bio-Oil from the Fast Pyrolysis of Mallee Bark. *Fuel*, **108**, 400-408. https://doi.org/10.1016/j.fuel.2012.12.018

[36] Jauhiainen, J., Conesa, J.A., Font, R. and Martın-Gullón, I. (2004) Kinetics of the Pyrolysis and Combustion of Olive Oil Solid Waste. *Journal of Analytical and Applied Pyrolysis*, **72**, 9-15. https://doi.org/10.1016/j.jaap.2004.01.003

[37] Alrawashdeh, K.A., Slopiecka, K., Alshorman, A.A., Bartocci, P. and Fantozzi, F. (2017) Pyrolytic Degradation of Olive Waste Residue (OWR) by TGA: Thermal Decomposition Behavior and Kinetic Study. *Journal of Energy and Power Engineering*, **11**, 497-510. https://doi.org/10.17265/1934-8975/2017.08.001

[38] Wzorek, M., Junga Ersel Yilmaz, E. and Bozhenko, B. (2021) Thermal Decomposition of Olive-Mill Byproducts: A TG-FTIR Approach. *Energies*, **14**, Article 4123. https://doi.org/10.3390/en14144123